

## Article

# Method of Site Selection and Capacity Setting for Battery Energy Storage System in Distribution Networks with Renewable Energy Sources

Simin Peng<sup>1</sup>, Liyang Zhu<sup>1</sup>, Zhenlan Dou<sup>2</sup>, Dandan Liu<sup>1</sup>, Ruixin Yang<sup>3</sup> and Michael Pecht<sup>4,\*</sup> <sup>1</sup> School of Electrical Engineering, Yancheng Institute of Technology, Yancheng 224051, China<sup>2</sup> State Grid Shanghai Integrated Energy Service Co., Ltd., Shanghai 200023, China<sup>3</sup> School of Mechanical Engineering, Beijing Institute of Technology, Beijing 100081, China<sup>4</sup> Center for Advanced Life Cycle Engineering (CALCE), University of Maryland, College Park, MD 20742, USA

\* Correspondence: pecht@umd.edu

**Abstract:** The reasonable allocation of the battery energy storage system (BESS) in the distribution networks is an effective method that contributes to the renewable energy sources (RESs) connected to the power grid. However, the site and capacity of BESS optimized by the traditional genetic algorithm is usually inaccurate. In this paper, a power grid node load, which includes the daily load of wind power and solar energy, was studied. Aiming to minimize the average daily distribution networks loss with the power grid node load connected with RESs, a site selection and capacity setting model of BESS was built. To solve this model, a modified simulated annealing genetic algorithm was developed. In the developed method, the crossover probability and the mutation probability were modified by a double-threshold mutation probability control, which helped this genetic method to avoid trapping in local optima. Moreover, the cooling mechanism of simulated annealing method was presented to accelerate the convergence speed of the improved genetic algorithm. The simulation results showed that the convergence speed using the developed method can be accelerated in different number BESSs and the convergence time was shortened into 35 iteration times in view of networks loss, which reduced the convergence time by about 30 percent. Finally, the required number of battery system in BESS was further built according to the real batteries grouping design and the required capacity of BESS attained using the developed method.

**Keywords:** battery energy storage system; site selection and capacity setting; genetic algorithm; simulated annealing algorithm



**Citation:** Peng, S.; Zhu, L.; Dou, Z.; Liu, D.; Yang, R.; Pecht, M. Method of Site Selection and Capacity Setting for Battery Energy Storage System in Distribution Networks with Renewable Energy Sources. *Energies* **2023**, *16*, 3899. <https://doi.org/10.3390/en16093899>

Academic Editors: Byoung Kuk Lee, Denis N. Sidorov and Paul Stewart

Received: 31 March 2023

Revised: 14 April 2023

Accepted: 3 May 2023

Published: 5 May 2023



**Copyright:** © 2023 by the authors. Licensee MDPI, Basel, Switzerland. This article is an open access article distributed under the terms and conditions of the Creative Commons Attribution (CC BY) license (<https://creativecommons.org/licenses/by/4.0/>).

## 1. Introduction

Compared to traditional fossil fuel energy, renewable energy sources (RESs) such as wind power and solar energy with the advantages of being less pollution were widely used in the practical application [1,2]. However, it might present challenges when the RESs are connected into the power grid with their timing characteristics [3,4]. Due to its advantages of high energy density and regulation accuracy, the battery energy storage system (BESS) can quickly realize the time-shifting of energy and resolve the power grid operation problems arising from the timing characteristics of RESs. It is an effective method to overcome the power grid connection problems arising from the RESs by BESS [5,6].

At present, many of efforts were made to research on how to realize the RESs grid-connection to the distribution networks using BESS and its site selection and capacity setting model. A three-layer optimal scheduling model of BESS is developed to determine the power scheduling scheme when the peaking economic benefit of thermal power plants is maximized [7]. In view of the stochastic volatility of wind power, a two-layer optimal configuration model for BESS is established to achieve a configuration scheme with minimal investing costs [8]. The ref. [9] developed a system cost model considering the cost of

deviating the power delivered to the grid and the cost of battery to determine the required battery. The ref. [10] presented an efficient cost reliability optimization model for optimal siting and sizing of BESS in the presence of responsible load management. The ref. [11] presented a mixed-integer non-linear programming model for solving the problem of optimal location, selection, and operation of BESSs and RESs in distribution system. The ref. [12] proposed an optimal planning of lithium ion BESS for microgrid application by considering the battery capacity degradation to minimize the sum of operating costs and energy storage costs.

These above-mentioned models of site selection and capacity setting of BESS, which are presented to minimize the BESS investment cost or maximize economic efficiency, are limited due to without considering on the distribution networks loss. Moreover, it is a hybrid non-linear planning problem to build a site selection and capacity setting model for BESS [13]. Many intelligent algorithms, such as genetic algorithms [14,15] and particle swarm algorithms [16], were widely used to solve BESS site selection and capacity setting model due to their advantages of global optimization and robustness. The ref. [17] developed a quantitative gravity inverse variable particle swarm algorithm to solve the capacity configuration scheme for a community hybrid BESS composed of retired power batteries and super capacitors. The ref. [18] presented a dimensional gravity center reverse mutation particle swarm algorithm to optimize configuration capacity of a hybrid energy storage system. The ref. [19] used a genetic algorithm to solve the multi-objective optimization for hybrid high energy and high power BESS to improve battery cycle life. Compared to traditional mathematical optimization algorithms, such as linear and non-linear planning methods [20,21], the above intelligent algorithms can solve the optimal configuration model of BESS. However, intelligent algorithms themselves have drawbacks, such as genetic algorithms with their fixed crossover and variance probabilities, which limit the scope of the algorithm's search for optimality, and the set of solutions obtained is usually not optimal, which leads directly to falling into a local optimum.

In this paper, a method based on simulated annealing genetic algorithm is developed to effectively attain site selection and capacity of BESS in distribution networks with RESs. The innovation of the developed method includes:

1. Developing a model, which includes constraints of BESS and minimizes the average daily distribution networks loss with a power grid node load;
2. To solve this model, a simulated annealing genetic algorithm, which consists of cooling mechanism of simulated annealing and double-threshold mutation probability control, is presented to accelerate the convergence speed and avoid trapping in local optima;
3. Based on the real grouping design of batteries and the optimal capacity of BESS attained by the developed method, the required number of battery system in BESS is attained to save the cost of BESS.

The rest of this paper is organized as follows: Section 2 presents the site selection and capacity setting model of BESS, Section 3 develops the simulated annealing genetic algorithm and solving the model by this algorithm, Section 4 discusses the simulation results used to verify the effectiveness and adaptive ability of the developed algorithm, and finally, Section 5 provides conclusions.

## 2. Siting Selection and Capacity Setting Model of BESS

### 2.1. Objective Function

In order to minimize the distribution networks loss, the average daily loss of the distribution networks with power grid node load should be minimized by an optimal configuration of BESS. The BESS, which is located at a node of the branch in the distribution networks, consists of three main parts: power conversion system, battery system, and battery management system. The battery system is composed of thousands of batteries which are connected in parallel and/or series to meet the capacity requirement of the BESS. The BESS is usually used to smooth the output power of RESs. To maintain the safety operation of the BESS, the state parameters of BESS, such as SOC and output power and

voltage, should be controlled to constraint values. The power grid node load includes the daily load of wind power and solar energy and the typical daily distribution networks load:

$$f = \min P_L = \min \left( \sum_{t=1}^T \sum_{a=1}^N I_a^2 Z_a \right) / T (a = 1, 2, 3 \dots N) \quad (1)$$

where  $P_L$  is the distribution networks loss,  $T$  is the time period,  $N$  is the total number of branches,  $I_a$  is the current of branch  $a$ , and  $Z_a$  is the impedance of branch  $a$ .

## 2.2. Constraint Condition

(1) Constraints of the node voltages in the distribution networks:

$$\begin{cases} U_{aL} < U_a < U_{aH} & a = 1, 2, 3 \dots n \\ U_{aH} \leq U_{bH} \end{cases} \quad (2)$$

where  $U_a$  is a node voltage,  $U_{aH}$  and  $U_{aL}$  are the upper and lower limit of a node voltage in the distribution networks, respectively.  $U_{bH}$  is the upper limit of BESS operating voltage, and  $n$  is the total number of distribution networks nodes.

(2) Constraints of branch currents and phase angles:

$$I_a \leq I_{aH}, a = 1, 2, 3 \dots N \quad (3)$$

$$\theta_L \leq \theta_a \leq \theta_H, a = 1, 2, 3 \dots N \quad (4)$$

where  $I_{aH}$  is the upper limit of  $a$  branch current  $I_a$ ,  $\theta_H$  and  $\theta_L$  are the upper and lower limits of phase angle  $\theta_a$ .

(3) Constraints of power flow of the distribution networks:

$$\begin{cases} P_{aD} - P_{aC} = U_a \sum_{b=1}^n U_b (G_{ab} \cos \theta_{ab} + B_{ab} \sin \theta_{ab}) \\ Q_{aD} - Q_{aC} = U_a \sum_{b=1}^n U_b (G_{ab} \sin \theta_{ab} - B_{ab} \cos \theta_{ab}) \end{cases} \quad (5)$$

where  $P_{aD}$  and  $Q_{aD}$  are the active and reactive power outputs of power injection nodes, respectively.  $P_{aC}$  and  $Q_{aC}$  are the active and reactive power loads at node  $a$ , respectively.  $U_a$  and  $U_b$  are the voltage amplitudes of node  $a$  and  $b$ , respectively.  $G_{ab}$  and  $B_{ab}$  are the real and imaginary parts of the node admittance matrix, respectively.  $\theta_{ab}$  is the voltage phase angle difference between node  $a$  and node  $b$ .

(4) Constraints of output power and state of charge (SOC) of BESS:

$$P_C \leq P_B \leq P_H \quad (6)$$

$$SOC_L \leq SOC \leq SOC_H \quad (7)$$

where  $P_B$  represents the output power of BESS,  $P_B > 0$  means discharge,  $P_B < 0$  means charge;  $SOC_L$  represents minimum SOC when BESS is discharged,  $SOC_H$  represents maximum SOC when BESS is charged.  $P_H$  indicates the maximum discharge power of BESS.  $P_C$  indicates the maximum charging power of BESS.

(5) Constraint of energy balance of BESS:

$$\int_0^T P_B(a) dt = 0 \quad (8)$$

(6) Constraint of power balance of the distribution networks:

$$P = \sum_{a=1}^n P_{e,a} - \sum_{g=1}^{n_g} P_{D,g} - \sum_{k=1}^{n_k} P_{B,k} \quad (9)$$

where  $P$  represents the power injected into the grid,  $P_{e,a}$  represents the load power of the  $a$ th node,  $P_{D,g}$  represents the output power of the  $g$ th Wind or Sloar,  $n_g$  represents the total number of Wind or Sloar connections,  $P_{B,k}$  represents the output power of the  $k$ th BESS unit.  $n_k$  represents the total number of BESS.

### 3. Modified Simulated Annealing Genetic Algorithm

The traditional genetic algorithm is usually limited by its disadvantages [22]. For example, due to its fixed step size, the convergence speed of this algorithm is too slow to save time. Moreover, it is easy for the algorithm to fall into local optimum because of its fixed crossover and mutation probabilities. In this paper, a modified simulated annealing genetic algorithm based on adaptive mechanism is presented:

1. A iterative temperature module based on cooling mechanism of modified simulated annealing is used to accelerate the convergence speed of the genetic algorithm;
2. To avoid trapping in local optimal solutions, the crossover probability and the mutation probability are modified randomly based on adaptive crossover probability, and adaptive double-threshold variation probability control. The control is present by the adaptive theory and the internal energy calculation formula of the simulated annealing algorithm.

#### 3.1. The Simulated Annealing Cooling Mechanism

For the traditional genetic algorithm, its iteration step is fixed. In this paper, the iterations condition of the genetic algorithm was replaced by the current iteration temperature ( $W_r$ ) based on the simulated annealing cooling mechanism. When the iteration step was changed by the simulated annealing cooling mechanism, the convergence speed of the genetic algorithm was accelerated. The simulated annealing cooling mechanism was realized as follows: Firstly, the initial temperature and the cooling rate and the maximum number of iterations were set, respectively. The initial temperature was used as the initial condition for the iteration process of the genetic algorithm. Secondly, the initial temperature decreased at the cooling rate in the iteration process, which changed the iteration step of the genetic algorithm. Finally, the iteration process of the genetic algorithm ended when the number of iterations reached the maximum number of iterations.

$$\begin{cases} W_0 = -q\Delta F / \ln Q_0 \\ \Delta F = F_m - F_l \\ W_r = W_0 * R^{T_e} \end{cases} \quad (10)$$

where  $W_0$  is the initial temperature of the iteration,  $q$  is the initial temperature coefficient,  $Q_0$  is a constant, and  $\Delta F$  is the fitness error;  $F_m$  and  $F_l$  are the maximum and minimum fitness values of the population individuals, respectively,  $T_e$  is the generations number of the current iteration, and  $R$  ( $0 < R < 1$ ) is the cooling rate.

#### 3.2. The Adaptive Crossover Probability and Adaptive Double-Threshold Variation Probability Control

The traditional genetic algorithm is easy to fall into the local optimal solutions because its crossover and variation probabilities are fixed, which limits the algorithm to find the optimal solution. In this paper, the adaptive crossover probability  $P_c$  and mutation probability  $P_m$  were modified by the adaptive mechanism. The  $P_c$  and  $P_m$  can be automatically adjusted according to the change of individual fitness value of the population.

$$P_c = \begin{cases} P_{c1} - \frac{(P_{c1}-P_{c2})(F-F_a)}{F_m-F_a}, F \geq F_a \\ P_{c1}, F < F_a \end{cases} \quad (11)$$

$$P_m = \begin{cases} P_{m1} - \frac{(P_{m1}-P_{m2})(F_a-F_j)}{F_a-F_m}, F_j \geq F_a \\ P_{m1}, F_j < F_a \end{cases} \quad (12)$$

where  $F$  is the individual with the greater fitness of the two current crossover individuals,  $F_a$  is the average fitness of the population individuals,  $F_j$  is the fitness of the current individual requiring variation,  $P_{c1}$  and  $P_{c2}$  are the maximum and minimum crossover probability, respectively,  $P_{m1}$  and  $P_{m2}$  are the maximum and minimum mutation probability, respectively, and  $P_{c1}, P_{c2}, P_{m1},$  and  $P_{m2}$  are all constants.

To expand the search range of the genetic algorithm for the optimal solution, a double-threshold mutation probability control based on the  $P_m$  and the simulated annealing mutation probability  $P_s$  is presented. The  $P_s$  was calculated using the simulated annealing internal energy expressed in Equation (13). The double threshold mutation probability control was realized as follows: Firstly, a real number  $G$  ( $0 \leq G \leq 1$ ) was randomly generated during variation operation of the genetic algorithm. Secondly, the  $G$  was compared with the mutation probability  $P_s$  and  $P_m$ , respectively, if the  $G$  was both smaller than the  $P_s$  and the  $P_m$ , the mutation operation of the genetic algorithm was carried out. Otherwise, the mutation operation of the genetic algorithm was not implemented. In the traditional genetic algorithm, the mutation operation was executed only when the  $G$  is smaller than the  $P_m$ .

$$\begin{cases} P_s = e^{-\frac{\Delta F_m}{W_r}} \\ \Delta F_m = F_m - F_j \end{cases} \quad (13)$$

where  $\Delta F_m$  is the individual fitness error.

### 3.3. Solving the Siting Selection and Capacity Setting Model Using the Developed Method

To solve the siting selection and capacity setting model, a chromosome  $(X_n, Y_n, Z_n)$  was generated, where  $X_n, Y_n$  and  $Z_n$  denote location and capacity and output power of the  $n$ th BESS in one cycle, respectively. Using the Newton–Lavson power flow method, the distribution networks loss in the siting selection and capacity setting model was calculated. Figure 1 shows the flow diagram of solving the siting selection and capacity setting model using the developed method.

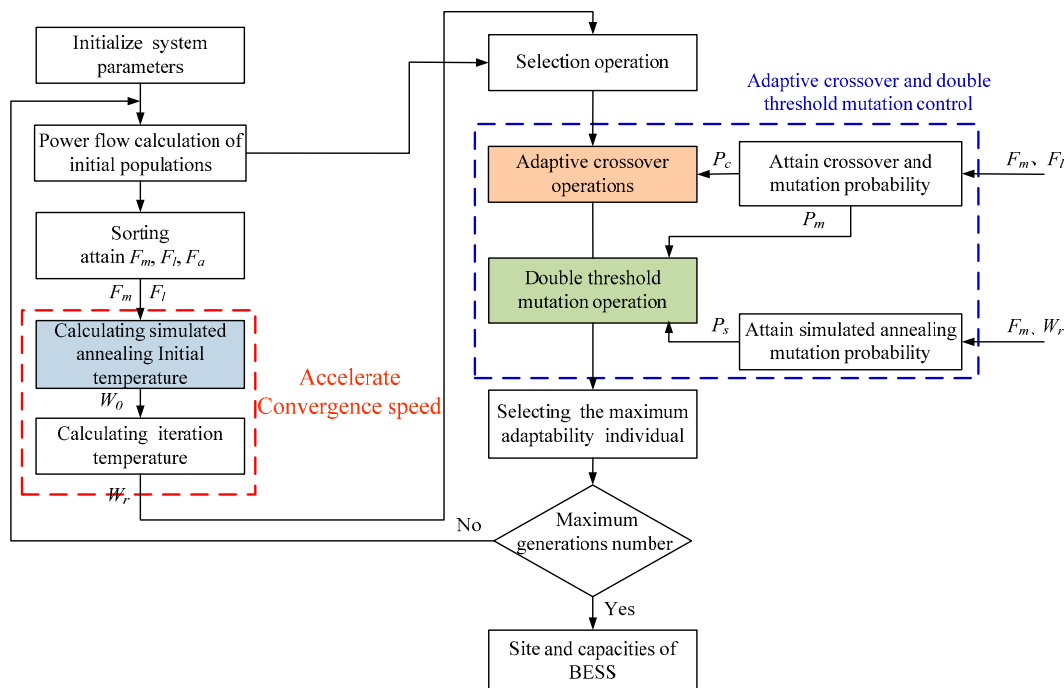


Figure 1. Flow diagram of solving the siting selection and capacity setting model using the developed method.

The solution process mainly included the following steps.

1. The system parameters are initialized, including binary code of the location, capacity and output power of BESS;
2. The power flow calculation based on the chromosome  $(X_n, Y_n, Z_n)$  is carried out to obtain the distribution networks loss by the Newton–Lavson power flow method. Then, the distribution networks loss is inverted as the initial population;
3. The initial population sorting operation is carried out to attain  $F_m, F_l, F_a$ ;
4. Initial temperature is calculated and the iteration temperature of the simulated annealing is used to accelerate the convergence speed of the genetic algorithm. The adaptive crossover probability and the double-threshold mutation probability control are used to accelerate the convergence speed;
5. The selection operation is carried out, and the adaptive crossover operation and the double-threshold mutation operation are performed to generate new populations;
6. Determines whether the iteration is completed. If the maximum generation number is reached, the site and capacity of BESS is attained; otherwise, go back to step (2).

#### 4. Simulation Results and Analysis

In order to verify the effectiveness and robustness of the developed method, a distribution networks system including IEEE33 nodes was studied. An amount of 400 kW solar energy and 300 kW wind power were connected at node 10 and node 18, respectively. The output power of wind power and solar energy and equivalent daily load are shown in Figure 2, respectively. The system simulation parameters are listed in Table 1. In this paper, only the active power of wind power and photovoltaic power generation were considered according to the real application.

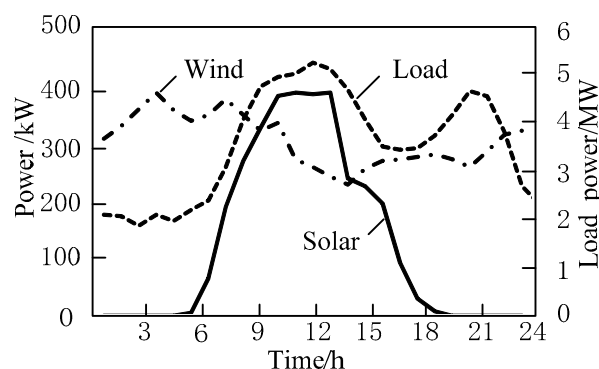


Figure 2. Output power of wind and solar and equivalent daily load.

Table 1. System simulation parameters.

Type of Algorithm	Parameter Name	Parameter Size	Parameter Name	Parameter Size
Genetic Algorithm	Population size	30	$P_c$	0.6
	$P_m$	0.01	Protection rate $P_p$	0.1
	Elimination rate $P_o$	0.1	Baseline power $S_b$	10 MVA
	Base voltage $V_b$	12.66 kV	Maximum number of generations	50
The developed method	$P_{c1}$	0.8	$P_{c2}$	0.6
	$P_{m1}$	0.2	$P_{m2}$	0.1
	$P_o$	0.6	$R$	0.995
	$B_0$	0.6	$q$	100
	$T$	24		

##### 4.1. Convergence Speed Analysis of the Proposed Method with Different Numbers of BESSs

To verify if the developed method can accelerate the convergence speed and shorten the convergence time compared to the traditional genetic algorithm, the average daily distribution networks losses were analyzed when different numbers of BESSs were connected to

the system nodes. Figure 3 shows average daily distribution networks losses with different number of BESSs. Figure 3a,b shows the variation of the daily distribution networks loss attained by the traditional genetic algorithm and the developed method, respectively.

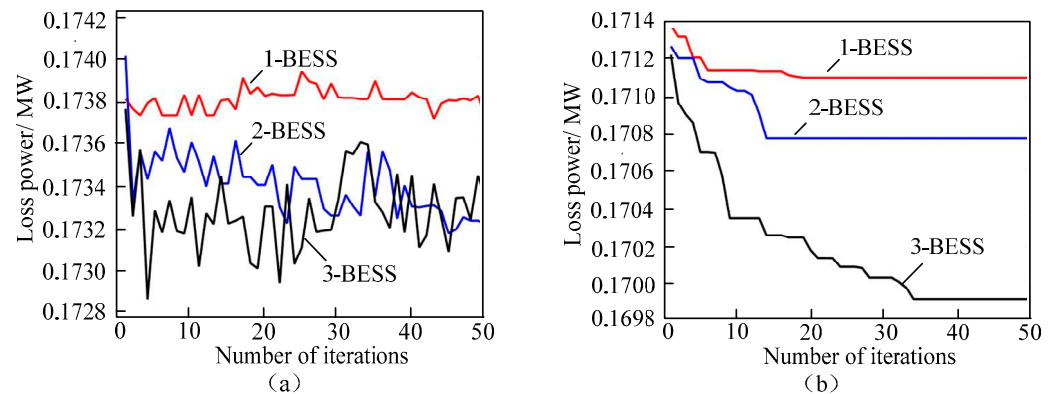


**Figure 3.** Average daily distribution networks losses with different number of BESSs: (a) Traditional genetic algorithm. (b) The developed method.

As shown in Figure 3, the networks losses generated by the developed algorithm were always lower than those networks losses generated by the traditional genetic algorithm. For example, when one, two, and three BESSs were connected to the system nodes, the average daily minimum networks losses using the traditional genetic algorithm were 173.72 kW, 173.17 kW, and 172.86 kW, respectively. However, the average daily minimum networks losses using the developed method were 171.8 kW, 170.77 kW, and 169.9 kW, respectively. The reason why the networks losses using the developed method were lower was that the developed algorithm can effectively expand the population research range by the adaptive mechanism and the double-threshold mutation probability control. It helps the developed method void falling into the local optimal solutions. On the other hand, it is clearly illustrated that the developed method can effectively accelerate the convergence speed and can shorten the convergence time. As shown in Figure 3a, the networks losses using the traditional genetic algorithm were in a state of flux or even variously divergent in 50 iterations. This was because the traditional genetic algorithm with a fixed iteration step should run its iterative process from 1 to the maximum number of iterations each time. To solve complex problems, such as obtaining this minimum networks losses, the traditional genetic algorithm will waste a lot of time to find the optimum due to its fixed iteration step. However, it can be seen from Figure 3b that all of the networks losses using the developed method can converge in 35 iterations, which reduces the convergence time by about 30 percent comparing to the traditional genetic algorithm. The developed method based on the improved cooling mechanism can adjust its iteration step to accelerate the convergence speed according to the adaptive change degree of the algorithm population. To sum up, the developed algorithm can effectively modify the convergence speed to shorten the convergence time in 30%. Meanwhile, it can be seen from Figure 3b that when three BESSs were connected the system nodes, the average daily distribution networks loss was at its minimum. In this case, the site and capacity of the BESS were attained with the capacity of 162 kWh, 200 kWh, and 179 kWh at node 18, node 12, and node 17, respectively.

Figures 4 and 5 show the variations of output power and SOC of BESS, respectively, when three BESSs were connected to the system nodes. The output power was positive power when BESS is discharging, and the output power was negative power when BESS was charging. As seen from these figures, at around 12:00 and 21:00, the loads demanded power in the distribution networks are higher, respectively. To keep the power balance of the distribute networks, each BESS discharged and supplied power to the distribution networks, and the SOC of each BESS was greatly reduced. In other times, due to the loads demand power in the distribution networks being lower, the BESSs were charged and the SOC of each BESS increased.

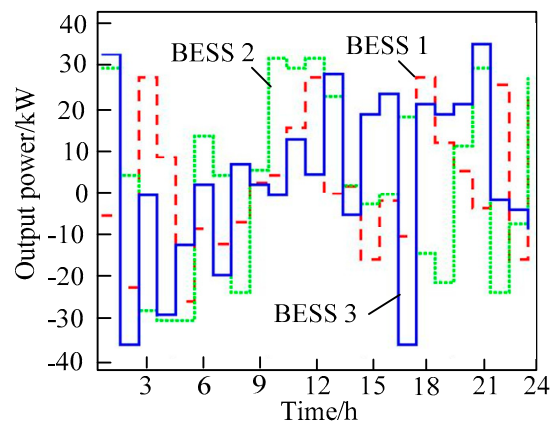


Figure 4. Output power of BESSs.

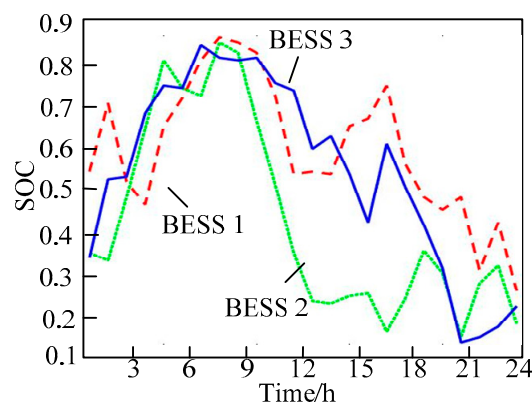


Figure 5. SOC of BESSs.

#### 4.2. Robustness of the Proposed Method with Different Crossover Probabilities and Variance Probabilities

To further verify the robustness of the developed method, the variations of the distribution networks losses were studied when the crossover probability  $P_c$  and mutation probability  $P_m$  were randomly modified with three BESSs connected the system nodes. The crossover and mutation probabilities were selected in three cases: In case 1, the crossover probabilities were kept constant and the mutation probabilities  $P_m$  were randomly selected as 0.02, 0.04, 0.06, and 0.07, respectively; in case 2, the mutation probabilities were kept constant and the crossover probabilities  $P_c$  were randomly selected as 0.3, 0.4, 0.7, and 0.8, respectively; in case 3, the crossover and mutation probabilities ( $P_c, P_m$ ) were changed simultaneously and selected as (0.4, 0.08), (0.5, 0.02), (0.7, 0.05), and (0.9, 0.07), respectively.

Figure 6 shows the average daily distribution networks losses when the crossover probability and the mutation probability were modified, respectively. Figure 6a–c shows the average daily distribution networks losses obtained by the conventional genetic algorithm with different mutation probabilities (Case 1), different crossover probabilities (Case 2), and different mutation probabilities and crossover probabilities, respectively (Case 3). As shown in Figure 6a,b, when the mutation probabilities and crossover probabilities were changed in different value, respectively, the average daily distribution networks losses based on the traditional genetic algorithm fluctuate greatly and still do not converge in 50 iterations. It means that the convergence performance of the networks losses based on the traditional genetic algorithm were very poor. Moreover, it can be seen from Figure 6c that, when the mutation probabilities and crossover probabilities were changed simultaneously, the variation trend of the networks losses were haphazard and did not go into a stepwise decline or even divergence in 50 iterations. It was further proved that the networks losses based on the traditional genetic algorithm change drastically or even fall into divergence due to its fixed crossover and variation probabilities. Figure 6d shows the average daily



distribution networks losses using the developed algorithm with different probabilities (Case 3). It is illustrated that the developed method can effectively control the convergence speed of the networks loss and the networks loss converged to a constant value (0.17 MW) in around 35 generations.

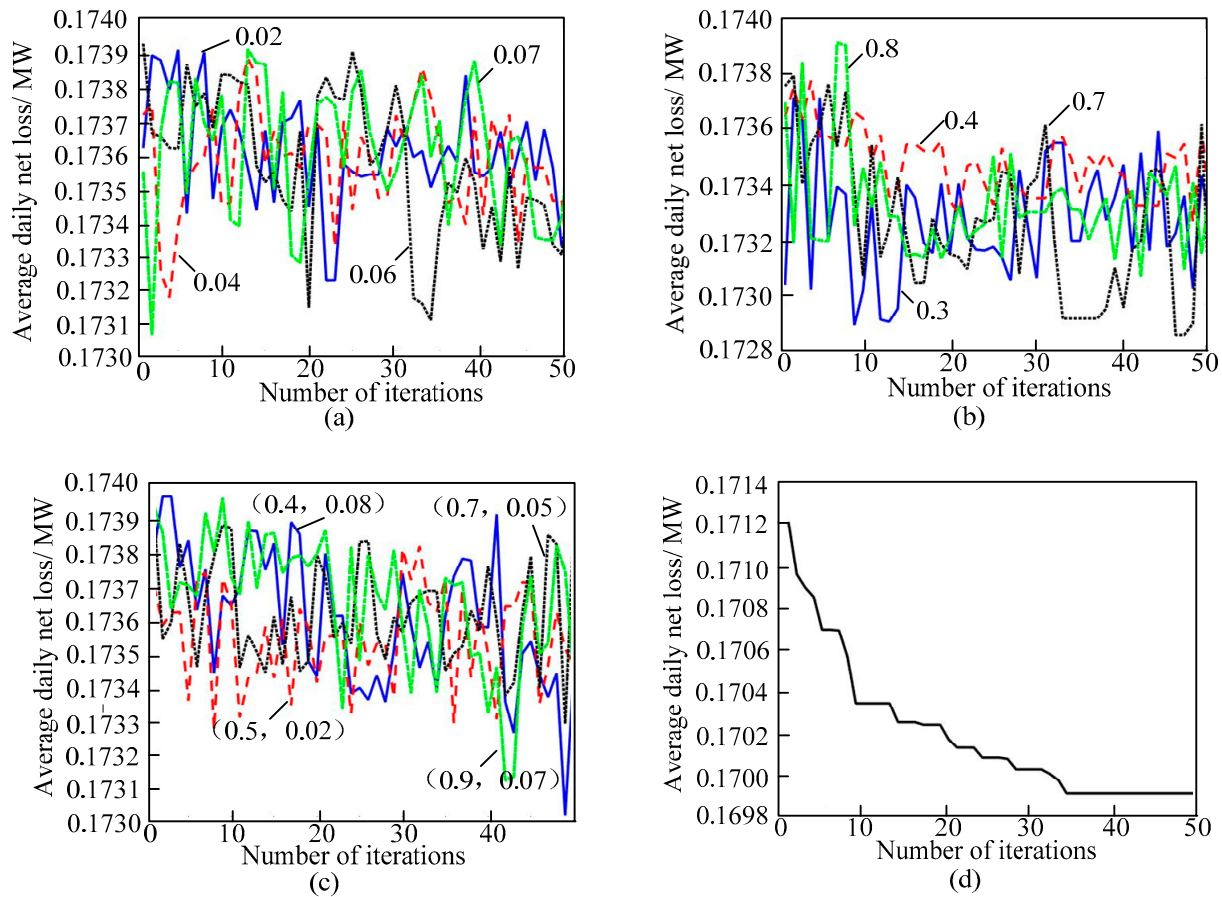


**Figure 6.** Average daily networks losses when the crossover probability and the variance probability are modified, respectively: (a) Different mutation probabilities (Case 1). (b) Different crossover probabilities (Case 2). (c) Different crossover and mutation probabilities (Case 3). (d) Networks loss using the developed method (Case 3).

Table 2 shows the average daily distribution networks losses of the system when the crossover and mutation probabilities were varied individually. Table 3 shows the average daily distribution networks losses when the crossover and mutation probabilities were modified together. The minimum average daily distribution networks losses using the developed method were always lower (169.9 kW) than the minimum one using the conventional genetic algorithm (173.06 kW). It means that the adaptive capability of the developed method was strong when the crossover and mutation probabilities were changed randomly.

**Table 2.** Average daily networks losses with different crossover probabilities and mutation probabilities separately.

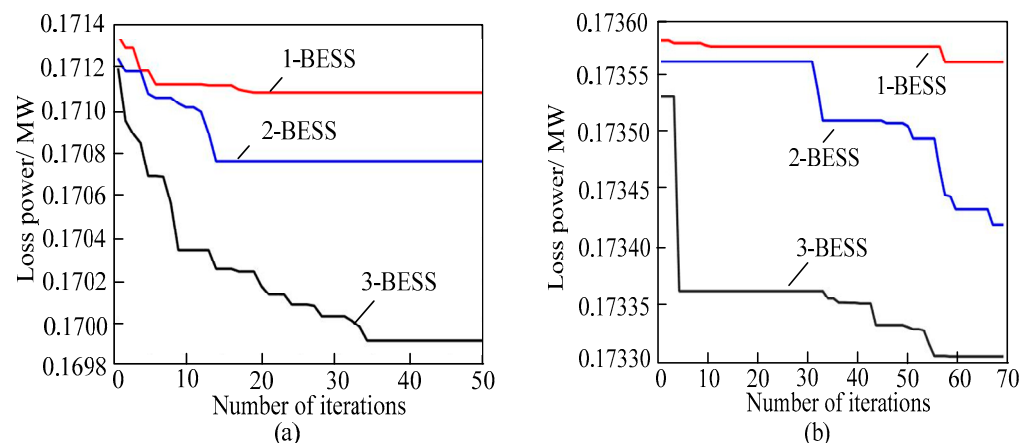
$P_c$	Genetic Algorithm/MW	$P_m$	Genetic Algorithm/MW	Developed Algorithm/MW
0.3	0.17292	0.02	0.17322	0.1699
0.4	0.17329	0.04	0.17317	
0.7	0.17289	0.06	0.1731	
0.8	0.1731	0.07	0.17306	

**Table 3.** Average daily networks losses with different crossover probabilities and mutation probabilities together.

$P_c$	$P_m$	Genetic Algorithm/MW	Developed Algorithm/MW
0.4	0.08	0.17302	
0.5	0.02	0.17327	
0.7	0.05	0.17329	0.1699
0.9	0.07	0.17312	

#### 4.3. Comparison of the Developed Method and the Simulated Annealing

To further verify the effectiveness of the developed method, a comparison of the developed method and the simulated annealing was conducted. As shown in Figure 7, the networks losses generated by the developed algorithm were always lower than those losses generated by the simulated annealing. For example, when one, two, and three BESSs were connected to the system nodes, the minimum networks losses using the developed method were 171.8 kW, 170.77 kW, and 169.9 kW, respectively. However, the minimum networks losses using the traditional genetic algorithm were 173.55 kW, 173.41 kW, and 173.32 kW, respectively. Moreover, it was clearly shown that the developed method can effectively accelerate the convergence speed and reduce the convergence time. Figure 7a shows that all of the networks losses using the developed method can converge before 35 iterations. However, as shown in Figure 7b, the networks losses based on the simulated annealing converged in about 60 iterations.

**Figure 7.** Comparison of the developed method and the simulated annealing with different number of BESSs: (a) the developed method. (b) The simulated annealing.

#### 4.4. Batteries Capacity Configuration Optimization of BESS

Using the developed algorithm, the optimal siting and capacity of BESS in the distribution networks can be attained. However, the grouping design and investment cost of the batteries should also be considered to further optimize the capacity of the battery system in BESS. From the above simulation results, it can be seen that the average daily distribution networks loss will be minimum when a BESS with optimized capacity (162 kWh, 200 kWh, 179 kWh) of batteries connected at nodes (18, 12, 17). In actual battery grouping design, a lithium iron phosphate battery with rated capacity of 200 Ah and a rated voltage of 3.2 V was selected to build a battery system (BS). The battery system was composed of many of battery clusters connected in parallel and the battery clusters were made up of many of battery modules in series, the battery modules consist of a lot of batteries. Considering the investment cost of batteries, the capacity configuration of the battery system in BESS connected to each node in the distribution can be designed as follows: one battery system with rated capacity of 192 kWh was composed of three battery clusters in parallel, one

battery cluster consisted of five battery modules in series, one battery module consisted of twenty battery cells in series. Two battery systems will be connected to BESS. Table 4 lists the capacity configuration options of batteries.

**Table 4.** Capacity configuration options of batteries.

Node Locations	Required Capacity/kWh	BS Rated Capacity/kWh	Required Number of BS
18	162	192	1
12	200	192	1
17	179	192	1

## 5. Conclusions

In this paper, a site selection and capacity sitting model of battery energy storage system (BESS) was established to minimize the average daily distribution networks loss with renewable energy sources. Due to considering many of operation constraints of BESS, such as the limit of operating voltage and output power and state of charge, the presented model is not only helpful to optimize the site selection and capacity sitting of BESS but to ensure the safe and reliable operation of BESS. To solve this model, a modified simulated annealing genetic algorithm, which was based on a cooling mechanism of simulated annealing and double-threshold mutation probability control, was presented. The effectiveness and adaptive ability of the presented algorithm was verified in distribution networks with the IEEE 33 node.

Compared to the traditional genetic algorithm, which has a fixed iteration step, the presented algorithm based on the cooling mechanism of simulated annealing can effectively accelerate the convergence speed and shorten the convergence time. In particular, the networks losses based on the developed method converged in 35 iterations when different numbers of BESSs were connected to the system nodes. On the contrary, the networks losses based on the traditional genetic algorithm tended to diverge.

With the help of the adaptive mechanism and the double-threshold mutation probability control, the developed method can not only avoid local optimal solutions, but exhibited higher robustness when the crossover probabilities and the mutation probabilities were modified randomly. In particular, when three BESSs were connected to system nodes, the average daily networks loss obtained by the developed algorithm (170 kW) was smaller than that of the traditional genetic algorithm (173 kW).

In a further study, an accurate battery model considering the state of health and depth of discharge of the battery will be established. Additionally, in the meantime, the economic benefits of the installing BESS should be inserted to the objective functions to construct a multi-objective BESS siting and capacity model. It will be of greater significance to guide the construction of the BESS in practical projects.

**Author Contributions:** All authors contributed to the study conception and design. Material preparation, data collection, and analysis were performed by all authors. Methodology, writing—review and editing, S.P.; writing—original draft preparation, data curation, visualization, L.Z.; project administration, validation, data curation, Z.D.; software, resources, methodology, D.L. and R.Y.; content organization and delivery, M.P. All authors have read and agreed to the published version of the manuscript.

**Funding:** We are grateful to the Jiangsu University “Qinglan Project” (2021-11), School-level research projects of Yancheng Institute of Technology (xjr2021052), and the National Grid Corporation Science and Technology Project of China (5400202140398A0000) for supporting this research.

**Institutional Review Board Statement:** Not applicable.

**Informed Consent Statement:** Not applicable.

**Data Availability Statement:** Not applicable.

**Acknowledgments:** The authors are very grateful to the reviewers, associate editors, and editors for their valuable comments and time spent.

**Conflicts of Interest:** The authors declare no conflict of interest.

### Abbreviations

The following abbreviations are used in this manuscript:

BESS	Battery energy storage system
RESs	Renewable energy sources
SOC	State of charge
BS	Battery system
$P_L$	The distribution networks loss

### References

1. Bilal, A.B.; Jin, W.J. Recent developments and future research recommendations of control strategies for wind and solar PV energy systems. *Energy Rep.* **2022**, *8*, 14318–14346.
2. Peng, S.; Zhu, X.; Xing, Y.; Shi, H.; Cai, X.; Pecht, M. An adaptive state of charge estimation approach for lithium-ion series connected battery system. *J. Power Sources* **2018**, *392*, 48–59. [[CrossRef](#)]
3. Akhilesh, G.; Manali, S.Z.; Hasan, M.M.F. Integration of cryogenic energy storage with renewables and power plants: Optimal strategies and cost analysis. *Energy Convers. Manag.* **2022**, *269*, 116165–116180.
4. Peng, S.; Chen, C.; Shi, H.; Yao, Z. State of charge estimation of battery energy storage systems based on adaptive unscented Kalman filter with a noise statistics estimator. *IEEE Access* **2017**, *5*, 13202–13212. [[CrossRef](#)]
5. Soliman, M.S.; Belkhier, Y.; Ullah, N.; Achour, A.; Alharbi, Y.M.; Al Alahmadi, A.A.; Abeida, H.; Khraisat, Y.S.H. Supervisory energy management of a hybrid battery/PV/tidal/wind sources integrated in DC-microgrid energy storage system. *Energy Rep.* **2021**, *7*, 7728–7740. [[CrossRef](#)]
6. Yu, Q.; Li, J.; Chen, Z.; Pecht, M. Multi-fault diagnosis of lithium-ion battery systems based on improved correlation coefficient and similarity approaches. *Front. Energy Res.* **2022**, *10*, 891637. [[CrossRef](#)]
7. Li, J.; Zhang, J.; Mu, G.; Ge, Y.; Yan, G.; Shi, S. Hierarchical optimization scheduling of deep peak shaving for energy-storage auxiliary thermal power generating units. *Power Syst. Technol.* **2019**, *43*, 3961–3970.
8. Sun, W.; Song, H.; Qin, Y.; Li, H. Energy storage system optimal allocation considering flexibility supply and demand uncertainty. *Power Syst. Technol.* **2020**, *44*, 4486–4497.
9. Gholami, M.; Shahryari, O.; Rezaei, N.; Bevrani, H. Optimum storage sizing in a hybrid wind-battery energy system considering power fluctuation characteristics. *J. Energy Storage* **2022**, *52*, 104634. [[CrossRef](#)]
10. Sayyad, N.; Majid, M.; Naser, N.E. An efficient cost-reliability optimization model for optimal siting and sizing of energy storage system in a microgrid in the presence of responsible load management. *Energy* **2017**, *139*, 89–97.
11. Alejandro, V.; Ricardo, A.H.; Ramon, A.G. Optimal location, selection, and operation of battery energy storage systems and renewable distributed generation in medium–low voltage distribution networks. *J. Energy Storage* **2021**, *34*, 102158.
12. Reza, F.; Mohsen, K. Optimal planning of lithium ion battery energy storage for microgrid applications: Considering capacity degradation. *J. Energy Storage* **2023**, *57*, 106103.
13. Yuan, Z.; Wang, W.; Wang, H.; Yildizbasi, A. A new methodology for optimal location and sizing of battery energy storage system in distribution networks for loss reduction. *J. Energy Storage* **2020**, *29*, 101368. [[CrossRef](#)]
14. Gu, T.; Wang, P.; Liang, F.; Xie, G.; Guo, L.; Zhang, X.P.; Shi, F. Placement and capacity selection of battery energy storage system in the distributed generation integrated distribution network based on improved NSGA-II optimization. *J. Energy Storage* **2022**, *52*, 104716. [[CrossRef](#)]
15. Deng, X.; Wang, F.; Hu, B.; Lin, X.; Hu, X. Optimal sizing of residential battery energy storage systems for long-term operational planning. *J. Power Sources* **2022**, *551*, 232218. [[CrossRef](#)]
16. Kerdphol, T.; Fuji, K.; Mitani, Y.; Watanabe, M.; Qudaih, Y. Optimization of a battery energy storage system using particle swarm optimization for stand-alone microgrids. *Electr. Power Energy Syst.* **2016**, *81*, 32–39. [[CrossRef](#)]
17. Li, Z.; Guo, K.; Liao, M.; Zhao, A.; Tian, M.; Wang, Y. Micro-hybrid energy storage system capacity based on genetic algorithm optimization configuration research. *Int. Core J. Eng.* **2020**, *6*, 78–83.
18. Su, H.; Yang, J.; Du, X.; Wang, Z.; Li, Y. Configuration of community hybrid energy storage system based on retired power battery. *Energy Rep.* **2020**, *6*, 934–942. [[CrossRef](#)]
19. Naseri, F.; Barbu, C.; Sarikurt, T. Optimal sizing of hybrid high-energy/high-power battery energy storage systems to improve battery cycle life and charging power in electric vehicle applications. *J. Energy Storage* **2022**, *55*, 105768. [[CrossRef](#)]
20. Zhu, X.; Xie, W.; Lu, G. Day-ahead scheduling of combined heating and power microgrid with the interval multi-objective linear programming. *High Volt. Eng.* **2021**, *47*, 2668–2679.

21. Timur, S.; Petr, V. Optimal utilization strategy of the LiFePO<sub>4</sub> battery storage. *Appl. Energy* **2022**, *316*, 119080.
22. Pandey, H.; Chaudhary, A.; Mehrotra, D. A comparative review of approaches to prevent premature convergence in GA. *Appl. Soft Comput. J.* **2014**, *24*, 1047–1077. [[CrossRef](#)]

**Disclaimer/Publisher's Note:** The statements, opinions and data contained in all publications are solely those of the individual author(s) and contributor(s) and not of MDPI and/or the editor(s). MDPI and/or the editor(s) disclaim responsibility for any injury to people or property resulting from any ideas, methods, instructions or products referred to in the content.